

REVIEWS

Open Access



Experimental study on the connection performance of single taper sleeve locking-type joint

Dongdong Li^{1,2,3,4*}, Tongheng Tu^{1,2,3,4}, Xiuli Yang^{1,2,3,4}, Maolin Cheng^{1,2,3,4} and Hao Xiao^{1,2,3,4}

*Correspondence:
239607323@qq.com

¹ CCCC Second Harbour Engineering Co. Ltd, Wuhan 430040, Hubei, China

² Key Laboratory of Transportation Industry for Long-Growth Bridge Construction and Building Technology, Wuhan 430040, Hubei, China

³ R&D Center of Intelligent Manufacturing Technology for Transportation Infrastructure in Transportation Industry, Wuhan 430040, Hubei, China

⁴ National Engineering Research Center for Long Bridge Construction of CCCC Highway, Beijing 100032, China

Abstract

In the pursuit of cost reduction and enhanced construction efficiency in the mechanical connection of reinforcing bars within precast assembled concrete structures, a novel-reinforcing bar connection joint is introduced. This innovative solution entails the utilization of 40Cr alloy steel tubing and the implementation of a hot forging high-precision rolling process to fabricate a series of new rebar joint specimens. Through unidirectional tensile testing, the failure modes of the specimens and the variations in load–displacement curves were meticulously analyzed. The investigation delved into the intricacies of the joint connection mechanism, scrutinizing the influence of three pivotal structural design parameters—namely the embedded length of the rebar, the sleeve thickness, and the clamp thickness—on the ultimate bearing capacity of the joint. The findings indicate that an embedded rebar length ranging from 1.5 to 1.75 times the nominal rebar diameter ensures a tensile strength ratio of the joint to the standard rebar tensile strength not less than 1.1. Notably, the sleeve thickness emerged as a significant factor impacting connection performance, while the clamp thickness exhibited negligible effects on specimen performance. Furthermore, an augmented internal thread angle was found to enhance shear resistance. The optimal design parameters encompass an outer sleeve diameter of 78 mm, a large end clamp diameter of 65 mm, and an internal thread angle of 60°. The proposed single taper sleeve locking-type joint, characterized by a rational structural design, aligns with the stipulations of Grade I joints outlined in the industry standard JG/J 107–2016. This novel joint design is well-suited for the mechanical connection of large-diameter rebars, offering a promising avenue for advancing construction practices in precast assembled concrete structures.

Keywords: New reinforcing steel joint, Mechanical connection, Mechanical property, Structural design, Failure mode

Introduction

The rapid economic growth in China has underscored the imperative for advancing construction industrialization. However, the industry faces critical challenges, including a scarcity of skilled labor in the low-end construction market, escalating labor costs, and inadequate mechanization. Notably, the steel reinforcement sector grapples with issues

of low productivity, heightened labor intensity, and limited mechanization, posing significant barriers to industry industrialization [1]. In recent years, a notable shift has been observed in the construction process, marked by the prefabrication of reinforcing steel components in factories, with a focus on green environmental practices and the adoption of assembly building projects. This transition has transformed the conventional approach of individual steel reinforcement connections into a product-based connection paradigm, leading to a substantial reduction in on-site personnel requirements, increased construction efficiency, and enhanced quality control within factory settings.

Within the realm of assembled buildings, the structural characteristics necessitate robust connections between prefabricated parts and other reinforced elements, which serve as primary load-bearing components and potential weak points within the structure. Consequently, the challenges associated with connections between prefabricated components assume paramount importance, as the mechanical properties of connector parts profoundly influence the overall structural safety and performance [2].

The proliferation of new Grade III reinforcing bars has catalyzed a surge in the utilization of high-strength, large-diameter reinforcing bars, propelling advancements in mechanical connection technologies towards enhanced quality, ease of construction, operational simplicity, and cost-effectiveness [3]. Building upon the evolutionary trajectory of sleeve cold extrusion, taper thread, and straight thread connections, the construction industry has witnessed the emergence of the fourth generation of rebar mechanical connection technology, tailored to the imperatives of industrialization. Noteworthy among these advancements are the taper sleeve locking joints, double screw sleeve joints, and U-set threaded joints, which have garnered prominence in the Chinese domestic landscape.

The double screw sleeve [4] reinforcing bar joint features a dual-layer design comprising inner and outer screw sleeves, effectively addressing the issue of non-collinearity in the trajectory line of the outer thread end of the reinforcing bar. However, its suitability is compromised in cases of radial deviation. In contrast, U-sleeve threaded joints excel in eliminating axial deviation but entail a more intricate installation process, with limited market applications. The tapered sleeve locking-type splicing (TSLTS) reinforcement joint emerges as a comprehensive solution to the aforementioned challenges, albeit at a higher cost [5].

Grouting sleeve joints are recognized for their reliability, yet ensuring joint quality poses challenges, making them more suited for “undisturbed influence” connection scenarios [6–8]. CADWELD melt-filled joints offer a viable solution for specific connection requirements, albeit demanding high-cost power supply provisions [9]. Conversely, MBT socket screw joints, wedge quick couplings, combined joints, and other foreign variants often fall short of meeting Chinese standard strength and deformation criteria, underscoring the need for tailored solutions within the local context.

The extruded locking connection technology, a novel generation of reinforcement bar mechanical connection technology collaboratively developed by the China Academy of Building Research and Qingdao Forest Metal Products Co. Ltd., represents a significant advancement in addressing the quality challenges associated with straight-threaded reinforcement bar connections, particularly in complex reinforcement bar sections [10]. This technology offers notable advantages in terms of simplicity, efficiency, and robustness,

making it well-suited for both standard connections and, notably, for the comprehensive connection of clustered reinforcement bars where rotation of the steel mesh, reinforcing steel cage, and prefabricated assembly structures is constrained [5]. Its alignment with the construction technology requirements of reinforcing steel components underscores its promising developmental trajectory.

Since its inception in 2015, there has been a paucity of research literature elucidating the operational mechanisms of extruded locking connection technology. Yang G. J. et al. [11] conducted mechanical performance assessments on tapered sleeve locking-type splicing reinforcement joint, validating their compliance with Class I joint standards as per regulations. These evaluations, encompassing unidirectional tensile tests and high-stress cyclic tension–compression tests, underscored the technology’s efficacy. However, existing studies have yet to delve into the intricate connection mechanisms of this technology or explore the impact of pertinent structural parameters on its connection performance, highlighting a critical research gap in the field.

To address the aforementioned challenges and advance the extruded locking connection technology under the partial construction process, this study introduces a novel single taper sleeve (STS) locking-type joint [12]. The STS locking-type joint aims to not only mitigate the costs associated with mechanical connection of reinforcing bars but also reduce the labor intensity inherent in the construction of assembled rebar connections, thereby propelling the development of extruded locking connection technology. In comparison to existing locking connectors, the STS locking-type joint features a simpler structure that facilitates easier installation, two bars to be connected without pretreatment, leading to time and cost savings in construction. By adopting a conventional machining approach, the processing costs are further reduced, enhancing the affordability of this technology. This innovation enriches the array of mechanical connection methods for reinforcing steel and introduces fresh perspectives for the connection of reinforcing steel components, as illustrated in Fig. 1.

Through a comprehensive analysis of the joint’s connection mechanism, this study identifies key structural design parameters that significantly influence the performance of rebar connections. Subsequently, unidirectional tensile tests are conducted on specimens to assess failure modes and evaluate the impact of each key design parameter on connection performance, thereby determining the optimal combination of structural

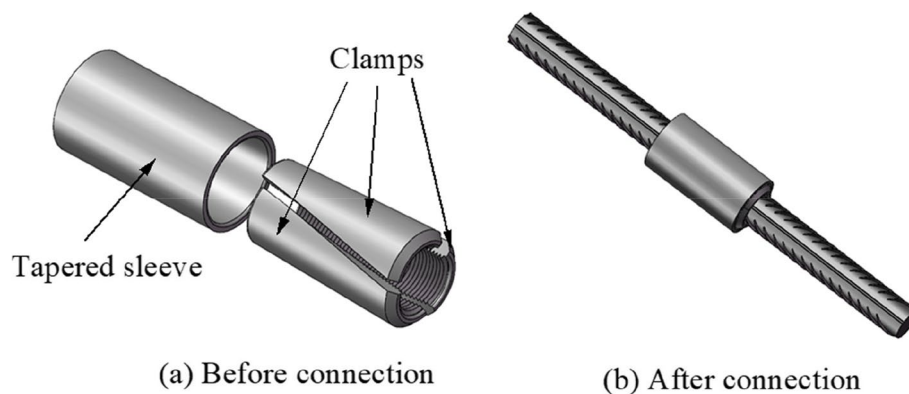


Fig. 1 STS locking-type joint

design parameters. Following this, specimens undergo rigorous high-stress repeated tensile and large deformation repeated tensile, to quantify residual deformations. These tests serve to validate the viability of the newly designed rebar connection joints for reinforcing steel bar connections.

Methods

Design of STS locking-type joint

Design requirements

- I. Adapt to the working condition that the rebar cannot rotate and the axial and radial deviation is within 2 cm.
- II. Applicable to HRB400E grade hot-rolled ribbed-steel bars with a nominal diameter of 40 mm
- III. Meet the industry standard of Grade I joints in the provisions of “Technical Regulations for Mechanical Connection of Reinforcing Steel Bars” JG/J 107–2016 [13].

External dimensions

A type of taper sleeve locking joint is proposed, namely single taper sleeve (STS) locking-type joint, which consists of a conical sleeve and a clamp. Among them, the overall shape of the clamp is conical, and with a taper angle of β , the end of its big end is equipped with a slope for easy installation, the length of the fit with the sleeve l_b is 130 mm, the overall length l_c is 140 mm, and the diameters of the small end d_{a1} as well as the large end d_{a2} are variable. The clamp is rotated and cut into three parts with a 55° helix angle, the inner surface is processed with M42 straight thread, the tooth angle is α , the pitch $P=3.2$ mm, and its size structure is shown in Fig. 2; the sleeve is wrapped around the clamp, its inner surface and the outer surface of the clamp are tightly adhered to each other, the inner surface is a conical hole and the outer surface is in the form of a whole cylindrical shape, and its size structure is shown in Fig. 3.

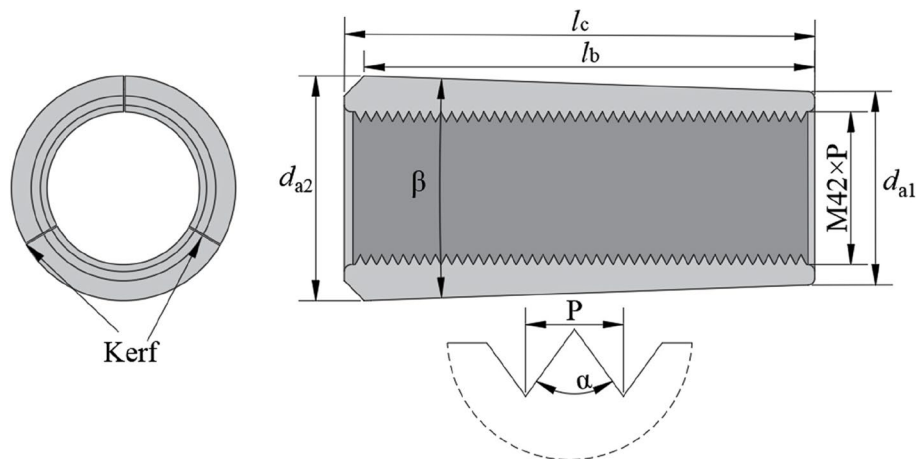


Fig. 2 Clamp structure sectional

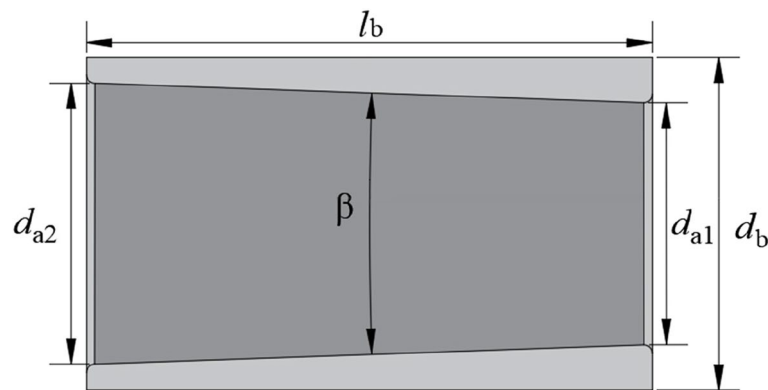


Fig. 3 Sleeve structure section

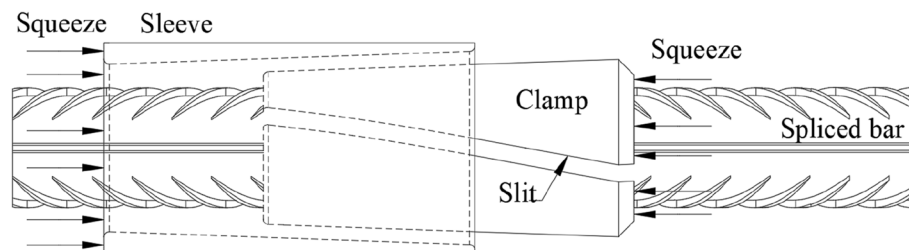


Fig. 4 STS locking-type joint pre-installation condition, arrow shows axially extruded sleeve

During the installation of STS locking joints, the initial step involves axially inserting the inner small end of the sleeve into one end of the rebar head. Subsequently, three clamps are radially positioned between the two bars intended for connection. Supported by auxiliary installation tools, the sleeve is axially squeezed. It is imperative to ensure that the position of the fixture should not be moved; when the sleeve moves axially, the fixture is subjected to radial extrusion pressure, radial locking of the rebar, to realize the connection of the rebar, as shown in Fig. 4.

Specimens

The specimen consists of two HRB400E hot-rolled ribbed bars with a nominal diameter (d) of 40 mm and STS locking-type joint, as shown in Fig. 5. Among them, according to the design requirements of the first steel joints, the connection of reinforcement bars was 55-mm, 57-mm, and 60-mm embedded length of the connection; ($l_a = l_d$) both sides of the symmetrical embedded in the internal reinforcement joints; clamp piece diameter of the large end d_{a2} of the 58 mm, 65 mm, 72 mm, respectively; sleeve by the outer diameter d_b of 69–85 mm made of steel tubes, respectively; and specimens of the structural design parameters of the specific combination of form as shown in Table 1.

Specimen materials

As per the findings in literature [14], it is evident that 40Cr alloy steel sleeves are suitable for connecting high-strength steel bars. Therefore, the materials chosen for the STS locking-type joint sleeves and clamps are 40Cr alloy steel, processed through hot forging

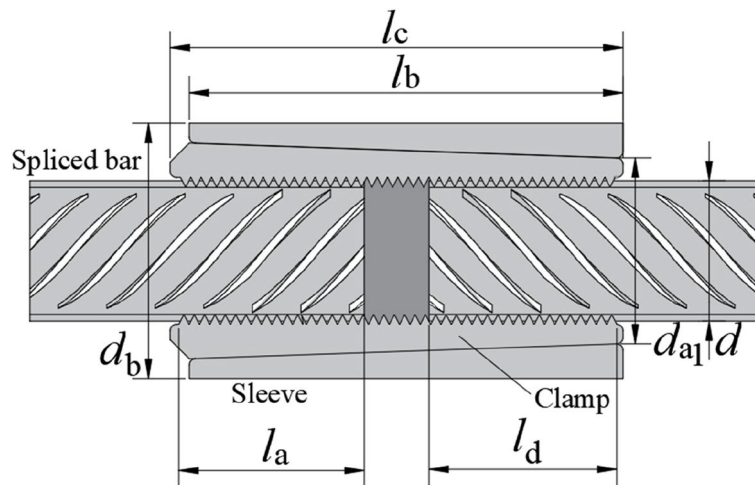


Fig. 5 Dimensional configuration of specimen

Table 1 Dimension of STS locking-type joint specimens

Specimen	Spliced bar		Sleeve				Clamp	
	l_a (mm)	d (mm)	d_b (mm)	l_b (mm)	d_{a1} (mm)	d_{a2} (mm)	a (°)	l_c (mm)
STS-1	55	40	69	130	56	65	55	140
STS-2	55	40	78	130	56	65	55	140
STS-3	55	40	85	130	56	65	55	140
STS-4	57	40	69	130	56	65	55	140
STS-5	57	40	78	130	56	65	55	140
STS-6	57	40	85	130	56	65	55	140
STS-7	60	40	69	130	56	65	55	140
STS-8	60	40	78	130	56	65	55	140
STS-9	60	40	85	130	56	65	55	140
STS-10	60	40	71	130	56	58	55	140
STS-11	60	40	85	130	56	72	55	140
STS-12	60	40	71	130	56	58	60	140
STS-13	60	40	78	130	56	65	60	140
STS-14	60	40	85	130	56	72	60	140
STS-15	57	40	71	130	56	58	60	140
STS-16	57	40	85	130	56	72	60	140

and high-precision rolling techniques, adhering to the industry standard “Sleeves for Mechanical Connection of Steel Reinforcement Bars” [15]. To assess the connection performance of large-diameter reinforcement bars, this study exclusively utilizes Grade III rebar: HRB400E ordinary hot-rolled steel bars with a nominal diameter (d) of 40 mm. The standard yield strength of these bars is 400 MPa, with an ultimate tensile strength of 540 MPa. In accordance with the standard “Steel for Reinforced Concrete Part 2: Hot Rolled Ribbed Steel Bar” [16], the mechanical properties of the test are evaluated, as presented in Table 2, detailing the steel reinforcement’s strength and mechanical characteristics. The results in Table 2 indicate that the ratio of measured tensile strength to yield strength exceeds 1.25, while the ratio of measured yield strength to standard yield

Table 2 Mechanical properties of specimen materials

Materials	Yield strength (MPa)	Ultimate tensile strength (MPa)	Modulus of elasticity (GPa)	Total elongation at maximum force (%)
40Cr alloy steel	785	980	206	-
HRB400E rebar	450	605	200	16

Test data are the average of three tests

strength is below 1.3, confirming that the mechanical properties of the reinforcement bars used in the test comply with the relevant regulations outlined in current Chinese national standards.

Test setup and loading method

The unidirectional tensile test, high-stress repeated tensile, and large deformation repeated tensile tests conducted in this study were executed using the MTS-1000-kN electro-hydraulic servo universal testing machine. The testing machine boasts a force value accuracy of 0.5% and is equipped with a computer screen for real-time display of test curves. The machine automatically extracts key parameters, such as maximum values, ultimate tensile strength, and yield strength, based on the input variables. The loading protocols for the aforementioned tests, detailed in Table 3, are applied until specimen failure occurs. The test loading apparatus is depicted in Fig. 6. Specific calculation formulas and measurement methods can be found in the JG/J 107–2016 specification [13].

Table 3 Test loading system

Pilot project	Loading system
Unidirectional tensile test	0 → 0.6 f_{yk} → 0 (measurement of residual deformation) → maximum tensile force (Record ultimate tensile strength) → devastation (determination of total elongation at maximum force)
High-stress repeated tensile test	0 → (0.9 f_{yk} → -0.5 f_{yk}) → devastation (20 repetitions)
Large deformation repeated tensile test	0 → (2 ϵ_{yk} → -0.5 f_{yk}) → (5 ϵ_{yk} → -0.5 f_{yk}) → devastation (Four repetitions) (four repetitions)

Load and deformation measurement deviation should not be more than ± 5%

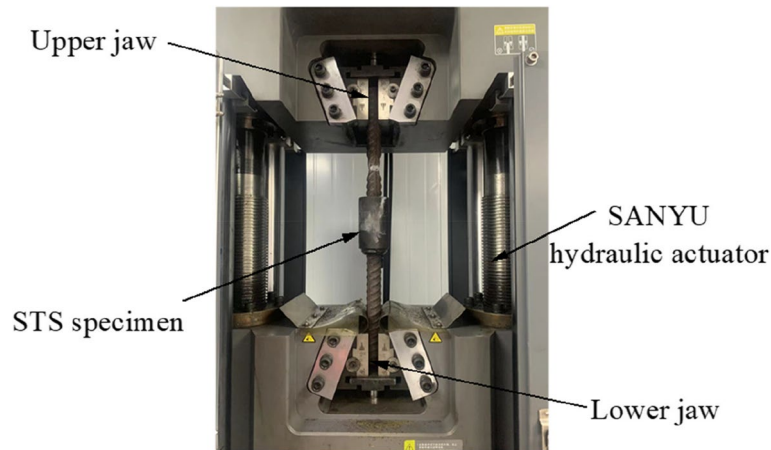


Fig. 6 Tensile test setup

STS locking-type joint connection mechanism

From the STS locking-type joint configuration, locking-type connector connection through the inner surface of the cleat pipe threads and the reinforcement bar transverse ribs, longitudinal ribs between the mechanical occlusal force and the sleeve and cleat ring binding force, the axial load from one end of the bar to the other end of the reinforcement bar. The structural connection load is transmitted through the reinforcements to the clamps, which further conveys the load to the sleeve. This process of force transfer primarily relies on the mechanical biting force generated by the threads between the reinforcements and the clamps, as well as the frictional force between the clamps and the sleeve.

Force analysis of sleeve and clamps

When subjected to axial tension, the rebar within the system depicted in Fig. 7 experiences a resultant stress perpendicular to the cone structure. The sleeve, in this configuration, plays a pivotal role by generating a stress that acts perpendicular to the cone. Frictional forces between the clamp and the sleeve contribute to the axial resistance stress, effectively countering a portion of the applied tensile force. Simultaneously, the radial force generated by this interaction establishes normal restraining stress, securing the bar and the clamp together to prevent detachment.

The oblique self-locking principle underscores the relationship between friction and the oblique cone angle $\beta/2$, indicating that a higher angle of inclination between the clamp and the sleeve enhances the sleeve's anchoring capacity for the clamp and the rebar. However, as the inclination angle increases, so does the necessary thickness of both the clamp and the sleeve. This escalation in dimensions leads to heightened production costs and may impede the ability to comply with steel construction requirements, particularly concerning the thickness of the protective concrete layer in certain scenarios.

The internal taper of the sleeve is the same as the external taper of the clamp when the connecting reinforcement is subjected to axial tension, the clamp connected to it will expand in all directions, and the reinforcement will produce uniform normal

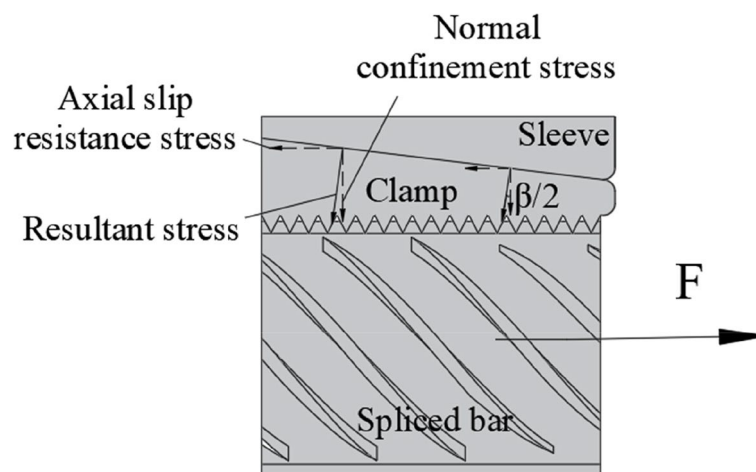


Fig. 7 Distribution of stress between sleeve and clamp

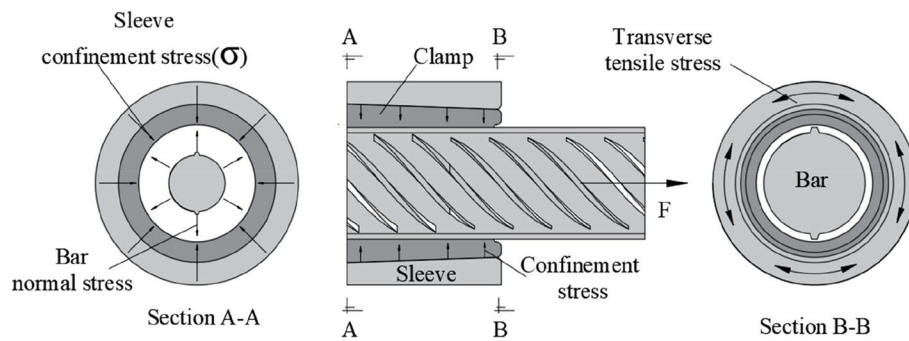


Fig. 8 Distribution of stress in STS locking-type joint. Section A-A, the bar was intentionally scaled down to make it easier to view the stress distribution

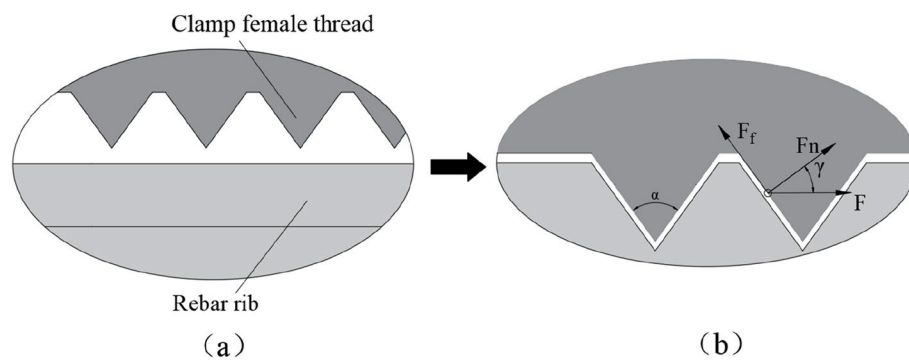


Fig. 9 Clamps and rebar force analysis. **a** Before connection. **b** After connection

stress along the periphery, and at this time, the confinement stress σ around the sleeve to resist the expansion of the clamp will be produced, which will firmly anchor the clamp and prevent it from dispersing and slipping. Regardless of whether the axial tension or compression is applied, the sleeve creates a confinement stress to stop the rebar from slipping in the axial direction (as shown in Fig. 8).

Forces analysis of clamp and rebar

During the installation process of the STS locking-type joint, the clamp undergoes radial extrusion pressure emanating from the circumference of the sleeve (Fig. 8). This pressure gradually forces the internal threads of the clamp to interlock with the transverse and longitudinal ribs present on the surface of the rebar. Consequently, the ribs of the rebar undergo plastic deformation, as illustrated in Fig. 9a to b. Notably, the ultimate tensile strength of the reinforcement joint material surpasses that of the reinforcement base material. Furthermore, the height of the internal threads does not exceed the height of the reinforcement ribs, thus ensuring the preservation of the reinforcement base material integrity. This process facilitates the achievement of an equal-strength connection.

After the installation of STS locking-type joint, the internal threads of the clamps are tightly attached to the rebar ribs, forming a threaded subconnection. Where $a = 2\gamma$, γ is the tooth bevel angle, which is known from the geometric relationship in Fig. 9:

$$F_n = \frac{F}{\cos\gamma} \quad (1)$$

$$F_f = \mu \cdot F_n \quad (2)$$

where F_n is the support force of the reinforcement base material on the threaded teeth of the clamp, F_f is the friction force of the reinforcement base material on the threaded teeth of the clamp, and μ is the friction coefficient between the reinforcement base material and the threaded teeth of the clamp.

From the literature [17], the threaded vice self-locking condition is as follows:

$$\tan\rho' = \mu/\cos\gamma \quad (3)$$

ρ' is equivalent friction angle, when the larger the tooth bevel angle (the larger the tooth angle), the larger the equivalent friction angle, the thread self-locking is better, the smaller the shear stress generated along the radially outward direction of the steel bar, and the connection performance is more favorable.

When the connected reinforcement is subjected to axial tension, the root of the thread is not only affected by tensile stresses σ but also by shear stresses τ caused by the radial deviation of the reinforcement. From the shear strain energy theory, it can be seen that when the value of $\sqrt{\sigma^2 + 3\tau^2}$ reaches the value of σ_y , the damage occurs. Set:

$$\sigma_v = \sqrt{\sigma^2 + 3\tau^2} \quad (4)$$

where σ_v is the equivalent force.

Consequently, damage occurs when the equivalent force σ_v in the part of the threaded sub-part formed by the rib of the rebar and the internal thread of the clamp reaches the value of the destructive stress σ_y induced by simple stretching in that portion.

When the connected reinforcement is subjected to an axial tensile force F , the tensile stress on the effective cross section of the threads on the reinforcement ribs, i.e., the restraining stress σ on the reinforcement by the sleeve (Fig. 8), is as follows:

$$\sigma = \frac{F}{(\pi/4)d_s^2} = \frac{4F}{\pi d_s^2} \quad (5)$$

where d_s is the equivalent diameter of the cross section of the thread stress on the rebar rib.

As shown in Fig. 10, before installation, the threaded sub is subjected to radial shear stresses due to the radial deviation between the two connecting bars, which creates a moment T . The moment-induced shear stress τ in the effective cross section of the threads on the rebar rib is as follows:

$$\tau = \frac{T}{(\pi/16)d_s^2} = \frac{8}{\pi} F \frac{d_p}{d_s^3} \text{tg}(\rho' + \gamma) \quad (6)$$

where T is the torque on the threaded pair and d_p is the equivalent diameter of the thread stress cross section in the clamp.

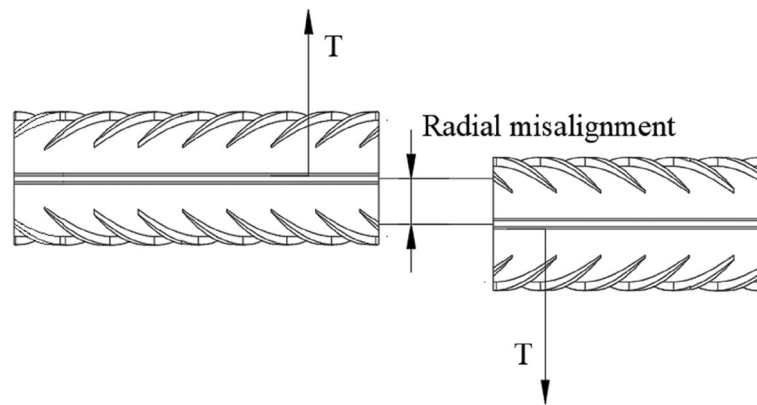


Fig. 10 Connection conditions with radial misalignment

Table 4 Unidirectional tensile test results of specimens (average of three specimens)

Specimen	f_{mst}^0 (MPa)	u_0 (mm)	A_{sgt} (%)	δ_u (mm)	Failure mode
STS-1	502	0.04	-	32	Bar pullout
STS-2	489	0.07	-	31	Bar pullout
STS-3	514	0.06	-	36	Bar pullout
STS-4	521	0.05	-	29	Bar pullout
STS-5	644	0.04	13.8	76	Bar fracture
STS-6	651	0.06	13.6	78	Bar fracture
STS-7	586	0.03	-	38	Bar pullout
STS-8	644	0.05	14.8	77	Bar fracture
STS-9	638	0.08	12.9	78	Bar fracture
STS-10	586	0.06	-	40	Clamp fracture
STS-11	641	0.07	13.7	77	Bar fracture
STS-12	591	0.05	-	37	Clamp fracture
STS-13	653	0.05	14.9	76	Bar fracture
STS-14	652	0.06	14.1	75	Bar fracture
STS-15	589	0.04	-	39	Clamp fracture
STS-16	667	0.06	13.6	76	Bar fracture

From the mathematical relationship of Eqs. 5 and 6 and the shear strain energy doctrine, it can be concluded that when the connecting reinforcement is subjected to axial tension, the restraining stress produced by the sleeve on the reinforcement is less than the value of the destructive stress caused by pure tensile, and the threaded threads may begin to break down, i.e., the STS locking-type joint will fail.

Results and discussion

Test results

The results of the unidirectional tensile test of the STS locking-type joint specimens are shown in Table 4, where f_{mst}^0 represents the ultimate tensile strength, u_0 represents the inelastic residual deformation, A_{sgt} represents the total elongation under the maximum force, and δ_u represents the failure displacement of the specimen.

Table 5 High-stress repeated tensile and large deformation repeated tensile test results (average of three specimens)

Specimen	f_{mst}^0 (MPa)	High-stress repeated tensile test	Large deformation repeated tensile test		Failure mode
		u_{20} (mm)	u_4 (mm)	u_8 (mm)	
STS-5	645	0.14	0.05	0.12	Bar fracture
STS-6	651	0.13	0.07	0.14	Bar fracture
STS-8	644	0.15	0.06	0.11	Bar fracture
STS-9	638	0.13	0.05	0.13	Bar fracture
STS-11	641	0.16	0.06	0.12	Bar fracture
STS-13	653	0.15	0.05	0.1	Bar fracture
STS-14	652	0.14	0.07	0.13	Bar fracture
STS-16	667	0.16	0.04	0.13	Bar fracture

Table 6 Ultimate bearing capacity and range of failure displacements in the form of failure

Failure mode	Specimen	Ultimate tensile strength f_{mst}^0 (MPa)	Failure displacement δ_u (mm)
Joint damage	STS-1, 2, 3, 4, 7, 10, 12, 15	489–591	29–40
Bar fracture	STS-5, 6, 8, 9, 11, 13, 14, 16	638–653	75–78

High-stress repeated tensile test and large deformation repeated tensile test are carried out on the specimen with the failure of rebar fracture, and the test results are shown in Table 5. The test results are shown in Table 5, representing the residual deformation after 20 times of high-stress repeated tensioning is indicated; u_4 and respectively the residual deformation after four times and eight times of large deformation repeated tensioning are indicated.

The results obtained from the unidirectional tensile test, high-stress repeated tensile test, and large deformation repeated tensile test (refer to Tables 5 and 6) reveal noteworthy insights. Specifically, an examination of specimen STS-5, 6, 8, 9, 11, 13, 14, and 16 demonstrates that their measured ultimate tensile strengths surpass the ultimate tensile strength of the connected steel bar. Additionally, the inelastic residual deformation remains below 0.14, while the total elongation under maximum force exceeds 6 units. Notably, after 20 cycles of repeated tensile testing, the residual deformation remains below 0.3. Furthermore, following four and eight repetitions of the tensile test, the residual deformation is less than 0.3 and 0.6, respectively. Moreover, the residual deformation post 20 cycles of high-stress repeated pulling and pressing is below 0.3. These results indicate compliance with the deformation requirements outlined for Class I joints as stipulated in the industry standard JG/J 107–2016 [13].

Failure mode

From the test results, it is observed that the proposed STS locking-type joint has two modes of failure: joint damage and bar fracture (Fig. 11c); among them, the joint damage includes clamp fracture (Fig. 11b) and rebar pullout (Fig. 11a).

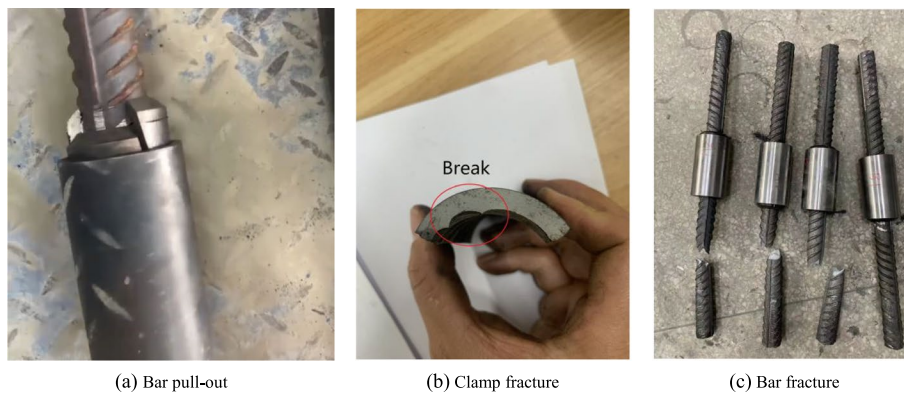


Fig. 11 Failure modes

The analysis of the ultimate bearing capacity range and failure displacements of the specimens detailed in Table 6 reveals significant observations when contrasted with the destructive failure mode of the connection. Firstly, specimens featuring fractured reinforcement exhibited enhanced tensile capacity, surpassing the ultimate tensile strength of the connected reinforcement. Secondly, a narrower range of variations in tensile strength was observed, underscoring the heightened reliability associated with the utilization of STS locking-type joints for connecting reinforcement bars. Lastly, the greater failure displacements noted predominantly stemmed from the elongation of the connected reinforcement bars post-yielding. These findings collectively suggest the superior performance and reliability of STS locking-type joints in reinforcing bar connections.

Behavior of STS locking-type joint

In the investigation of the ultimate load carrying capacity of rebar connectors, numerous influencing factors come into play. However, this study focuses solely on examining the impact of rebar embedding length, clip thickness, and sleeve thickness on the connection performance of STS locking-type joints within the framework of the principal design of STS locking-type joint.

Figure 12a shows the load–displacement response curves of the specimens with rebar embedded lengths of 55 mm, 57 mm, and 60 mm, respectively. In the unidirectional tensile test of specimens STS-5 and STS-8, the whole connection structure is in the elastic deformation stage at the initial loading, and the displacement is very small at this time, and no obvious deformation is observed in the components at this stage; with the further increase of the load applied by the universal testing machine, the specimen gradually enters into the yielding stage at a load of about 550 kN, and the point A in the figure is the yielding point, that is, the increase of load is very small, and the displacement of the specimen increases significantly. There is an obvious yielding region, and it can be clearly seen that the specimen then gradually yields. Very small, the specimen displacement increased significantly.

In Fig. 12a, there is a clear yield region, which can be clearly seen after the specimen and then gradually yield; there is a clear point of rise, and then gradually stabilized; and the peak load was 782 kN and 791 kN. Thereafter, the steel bar is subjected to greater than their own tensile strength of the load, and the occurrence of brittle fracture, in the

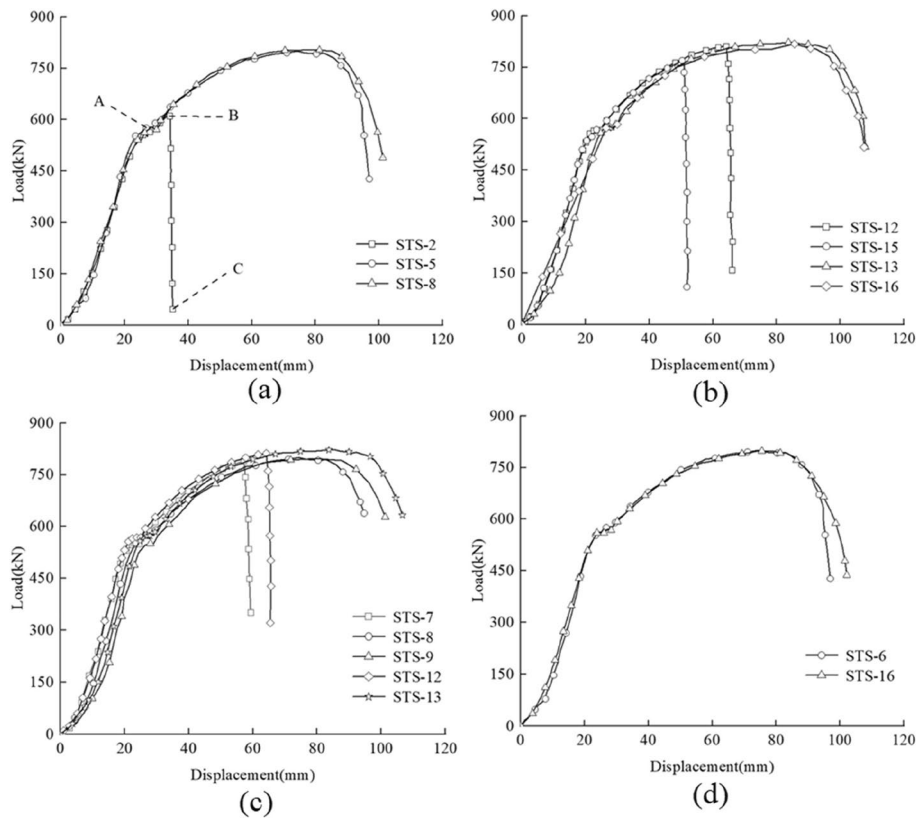


Fig. 12 Load–displacement graph

figure, shows a downward trend. As for the STS-2 specimen, the embedded length is 55 mm, and the effective contact area between the internal threads of the clamping piece and the ribs of the reinforcement is reduced, which makes it difficult to resist the larger axial load, and the peak load is only 610 kN, and after yielding, it fails in the form of reinforcement slipping and shows a nearly vertical straight line (BC) decline in the graph.

Therefore, the embedment length of the connecting reinforcement has a significant effect on the connection performance of the specimen. The larger the embedding length, the larger the peak displacement, i.e., the longer the reinforcement phase of the specimen, indicating that the specimen has a stronger ability to resist damage. Such as specimen STS-5, when the embedded length is 57 mm, its axial deviation is greater than the design requirements (20 mm) and also meets the standard of Class I joints; for STS taper sleeve locking joint, the embedded length of the reinforcement should not be less than 1.5-d length.

Figure 12b shows the unidirectional tensile test load–displacement response curves of specimens with three different clamp diameters. When the diameter of the small end of the clamp d_{a1} is certain, the larger the diameter of the large end of the clamp d_{a2} is, the larger the angle of inclination of the outer surface of the clamp is, the thicker the clamp is, and the increase of the angle of inclination, the radial component of the restraining stress acting perpendicularly to the inclined plane, is enough to resist the axial load, but blindly increasing the taper is not desirable either.

For the specimens STS-13 and STS-16, when the diameter of the large end of the clamp d_{a2} is increased from 65 to 72 mm, its tensile strength is increased from 653 to 667 MPa, and the tensile capacity is improved, but the clamp is too thick, which means that the cost of steel joints is increased, which is also not desirable. Taking the specimens STS-12 and STS-15, which failed by rebar fracture, their corresponding clamps have a diameter of 58 mm at the big end, and the clamps are too thin, and they will fracture (Fig. 11b). The results show that it can be seen that the thickness of the clamps does not have a significant effect on the ultimate load carrying capacity.

Figure 12c shows the load–displacement response curves of the specimens with different sleeve OD. d_b . The STS-7 with 69-mm sleeve OD and the STS-12 with 71-mm sleeve OD are both in the connection damage failure mode, with a peak load of nearly 800 KN, and the sleeve ruptures in the strengthening stage, followed by a straight-line decline. With the specimens of steel bar fracture failure, its curve includes elastic stage, yield stage, strengthening stage, and damage stage, from the curve trend, with the increase of the outer diameter of the sleeve, i.e., the thicker the sleeve, the greater the ultimate load carrying capacity of the specimen, the tensile strength will be increased, but the difference is not great. Therefore, the thickness of the sleeve on the ultimate bearing capacity of the specimens of the impact is more significant, the sleeve which is too thin will be connected to the rupture and failure, the sleeve is too thick, it will increase the processing cost, and in some cases, it is more difficult to meet the requirements of the thickness of the concrete protective layer.

Figure 12d illustrates the load–displacement response curves of the test piece for two different angles of the internal threaded teeth of the clamp. From the test results, it can be seen that there is no significant change in the ultimate bearing capacity when the angle of the internal threaded teeth of the clamping piece is changed from 55 to 60°.

Conclusions

This paper investigated the effects of the geometrical shapes of a new type of reinforcing bar connection joint. STS locking-type joint, in providing solution to splice two steel bars under tensile load. It allows stress to be transferred among the bar, clamps, and the sleeve, and under the confinement provided by the conical sleeve, better connection performance is ensured.

The findings of the study are obtained from experimental tests of the single taper sleeve locking-type joint with the bar embedded length ranging from 55 to 60 mm, the diameter of the large end of the clamp ranging from 58 to 72 mm, and the sleeve OD ranging from 69 to 85 mm. The proposed structural design of STS locking-type joint is reasonable and complies with the corresponding index provisions of Grade I joints in the industry standard JG/J 107–2016. However, for the reason that tensile test was conducted on bars with 40-mm diameter only, the findings are applicable for the bar size only, at least for the time being.

Nevertheless, the test results provide valuable data on the effects of the diameter of the large end of the clamp and the sleeve OD and bar embedded length to the performance of STS locking-type joint, where increase in bar embedded length and sleeve OD will improve the connection performance. However, the effect of the large end diameter of the clamps on the ultimate bearing capacity is not significant. When the large end

diameter of the clamps is increased from 65 to 72 mm, the ultimate load carrying capacity increases by only about 2%.

From the test results, the sleeve OD and the bar embedded length of the STS locking-type joint provide significant effects on connection performance. Increase of sleeve OD from 69 to 85 mm leads to an increment of approximately 9% higher ultimate bearing capacity. Meanwhile, as the bar embedded length increases from 55 to 60 mm, the ultimate bearing capacity of the STS locking-type joint increases approximately 32%. In addition, within a certain range, the angle of the internal threaded teeth of the clamp is increased for greater shear resistance.

When the embedded length of rebar is 1.5–1.75 d , the diameter of the large end of the clamp is 65 mm, the sleeve OD is 78 mm, and the angle of the inner thread of the clamp is 60°; the ultimate bearing capacity of the STS joint is the largest, and the connection performance is the best.

Abbreviations

STS	Single taper sleeve locking-type joint
HRB	Hot-rolled ribbed-steel bar
TSLTS	Tapered sleeve locking-type splicing
CAD	Computer-aided design
°	Degree
Mm	Millimeter
MPa	Megapascal
GPa	Gigapascal
MTS	MTS Systems Corporation
KN	Kilonewton
OD	Outside diameter

Acknowledgements

Not applicable.

Authors' contributions

DL completed the structural design of the rebar joints, TH conceptualized and done the experimentation, XY analyzed the connection mechanism of rebar joints, MC performed data curation and editing, and HX interpreted and visualized the data. All authors have read and approved the final manuscript.

Funding

The authors would like to acknowledge the financial supported by the National Key Research and Development Program of China (No. 2022YFB2302500).

Availability of data and materials

The data used to support the findings of this study are included within the article and are available from the corresponding author upon request.

Declarations

Competing interests

The authors declare that they have no competing interests.

Received: 11 September 2023 Accepted: 24 March 2024

Published online: 03 April 2024

References

- Zhang S. Research on the development of China's construction industrialization in the context of the new era [D]. Tianjin University, 2016. <https://doi.org/10.7666/d.D01158633>.
- Song L. Research on mechanical properties of new forged grouting sleeve connection [D]. Anhui University of Technology, 2022. <https://doi.org/10.26918/d.cnki.ghngc.2022.000088>.
- Liu ZJ. Current status and development trend of rough steel bar connection technology [J]. Construction Mechanization 2000 (06):28–29. <https://doi.org/10.13311/j.cnki.conmec.2000.06.011>.
- Xu RR, Wang KY. A "dry" reinforcing bar mechanical connection technology in precast assembled structures[C]. // Proceedings of the 8th China (International) Precast Concrete Technology Forum. 2018:166–169.

5. Xu RR, Tian CY, Wang XM, et al. Taper sleeve locking reinforcement connection technology and its application in assembled concrete structures[C]. // Proceedings of the 5th China (International) Precast Concrete Technology Forum. 2015:156–160.
6. Xu F, Wang K, Wang S et al (2018) Experimental bond behavior of deformed rebars in half-grouted sleeve connections with insufficient grouting defect[J]. *Constr Build Mater* 185:264–274
7. Chen J, Wang Z, Liu Z et al (2020) Experimental investigation of mechanical behavior of rebar in steel half-grouted sleeve connections with defects in water/binder ratio[C]//Structures. Elsevier 26:487–500
8. Ling JH, Rahman ABA, Ibrahim IS et al (2012) Behavior of grouted pipe splice under incremental tensile load[J]. *Constr Build Mater* 33:90–98
9. Randolph HT (1979) Quality control of CADWELD (Mechanical) Splices[J]. *J Construct Div* 105(3):201
10. Wang J, Wang Z, Du J (2023) Corrosion characteristics of tapered sleeve locking-type splicing reinforcement in precast segmental bridge piers[C]//Structures. Elsevier 48:1907–1919
11. Yang GJ, Li Y, Zhao RN et al (2021) Experimental study on the mechanical properties of new type of large-diameter rebar taper sleeve locking mechanical joint[J]. *Sichuan Construct Sci Res* 47(03):50–55. <https://doi.org/10.19794/j.cnki.1008-1933.2021.0034>
12. Zhang YT, Zhang H, Tian W et al. A single cone type rebar connector and its connection method [P]. Hubei province: CN115928941A, 2023–04–07.
13. JG/J 107–2016, Technical specification for mechanical connection of steel bars [S].
14. Li XM, Wang Y, Gao RD et al (2017) Experimental study on mechanical properties of mechanically connected joints of high-strength steel bars[J]. *Industr Construct* 47(12):148–151
15. JG/T 163–2013, Sleeves for mechanical connection of steel bars [S].
16. GB/T 1499.2–2018, Steel for reinforced concrete Part 2: Hot-rolled ribbed steel bars [S].
17. Xing HN. Research on mechanical behavior of direct threaded sleeve connection of steel bars and its application [D]. Dalian University of Technology, 2004. <https://doi.org/10.7666/d.y666263>.

Publisher's Note

Springer Nature remains neutral with regard to jurisdictional claims in published maps and institutional affiliations.